

# *Constrained time-lapse inversion of 3-D resistivity surveys data*

**M.H.Loke (Geotomo Software)**

**T. Dahlin & V. Leroux (Lund University)**

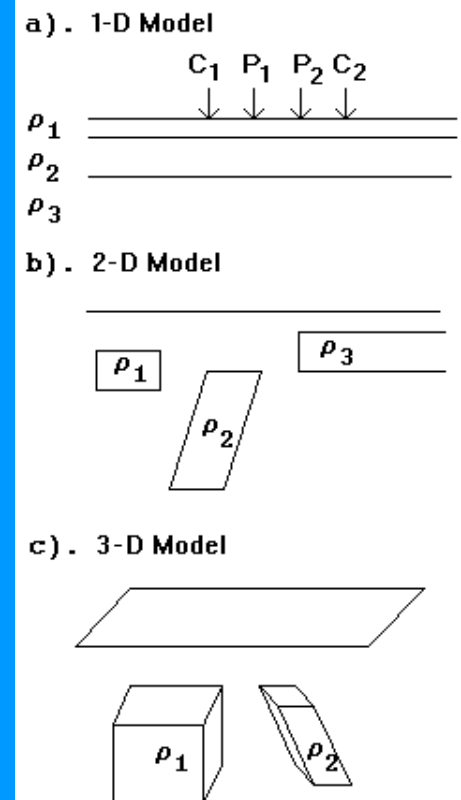
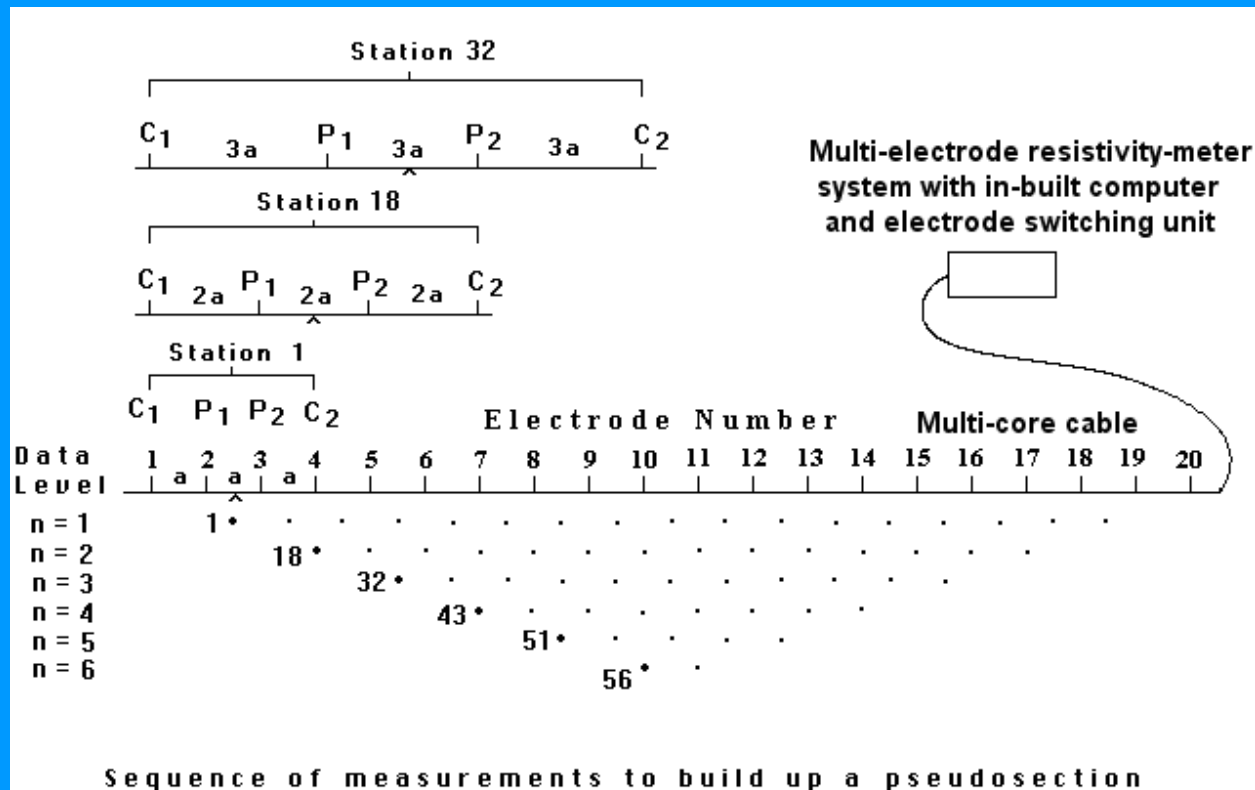
*Email : [drmhloke@yahoo.com](mailto:drmhloke@yahoo.com)*

# Outline

1. From 2-D to 3-D electrical imaging surveys
2. Least-squares inversion in space and time
3. Synthetic model example
4. Landfill field survey
5. Water irrigation experiment
6. Conclusions

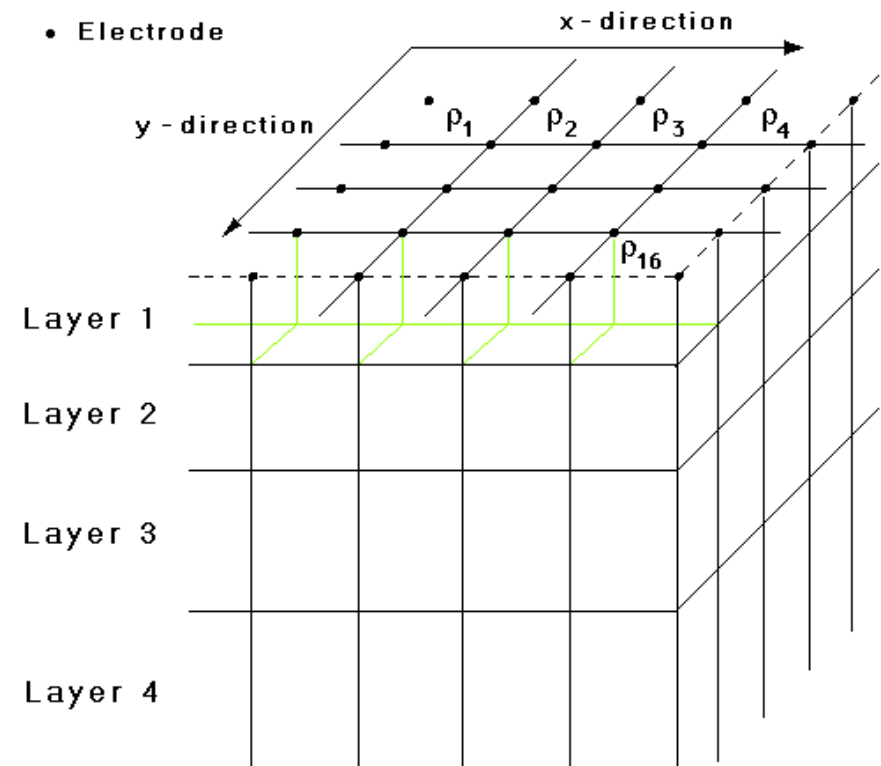
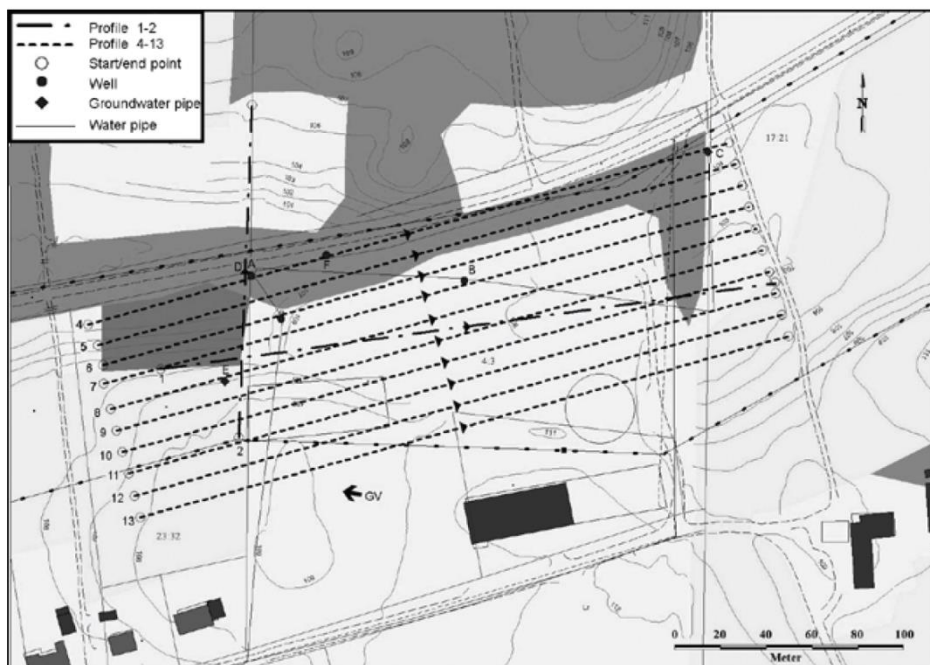
## 2-D electrical imaging surveys

2-D electrical imaging surveys are now widely used. However, in very complex environments, a 2-D model might not be sufficiently accurate due to off-axis structures. Our interest is in mapping temporal changes from repeated 3-D surveys.



# Types of '3-D' surveys and models – simple case

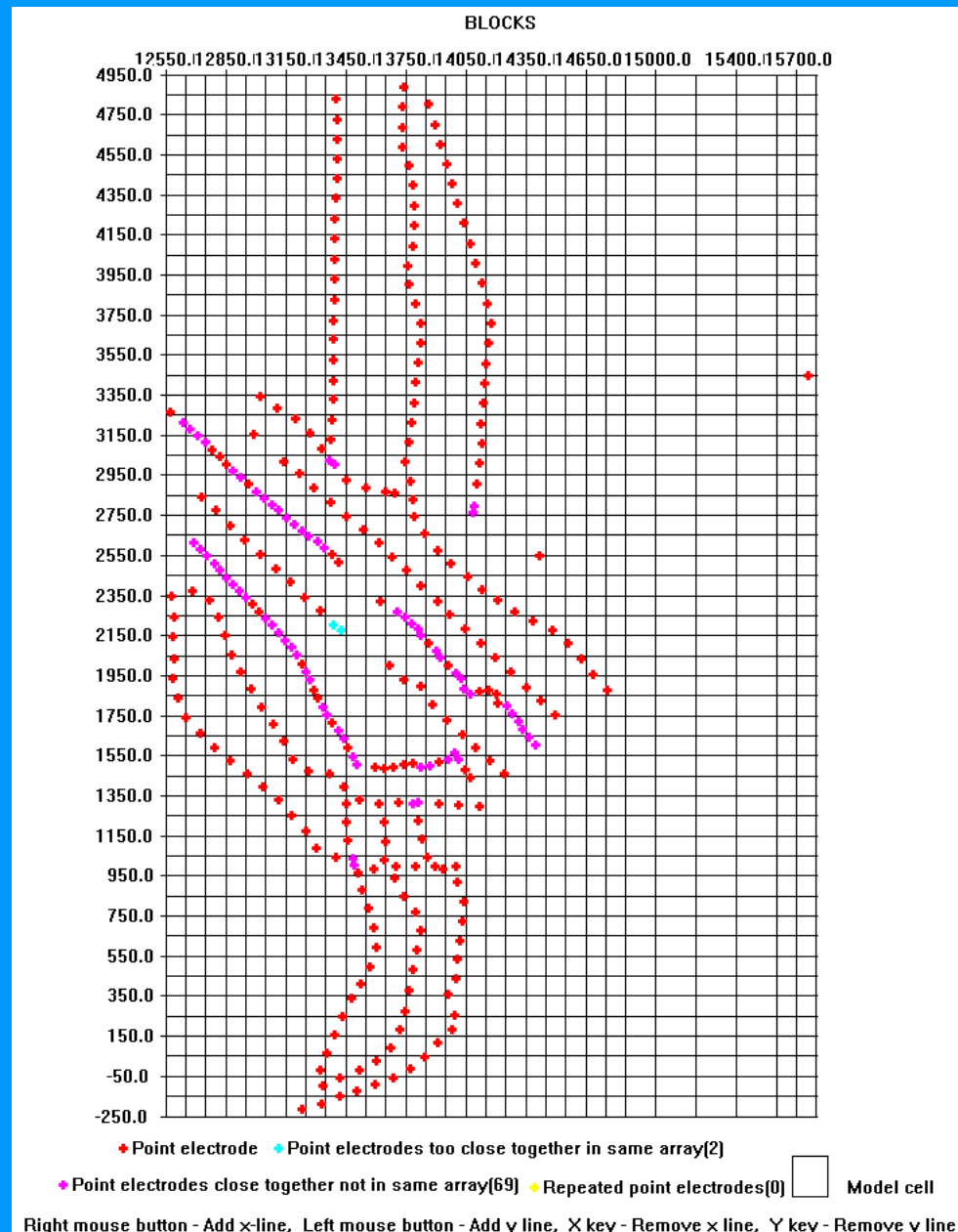
The simplest type is with parallel 2-D surveys lines. The positions of the electrodes provide a 'natural' means to subdividing the subsurface model into rectangular blocks. The corners of the blocks are set by the positions of the electrodes.



# Types of '3-D' surveys and models – complex cases

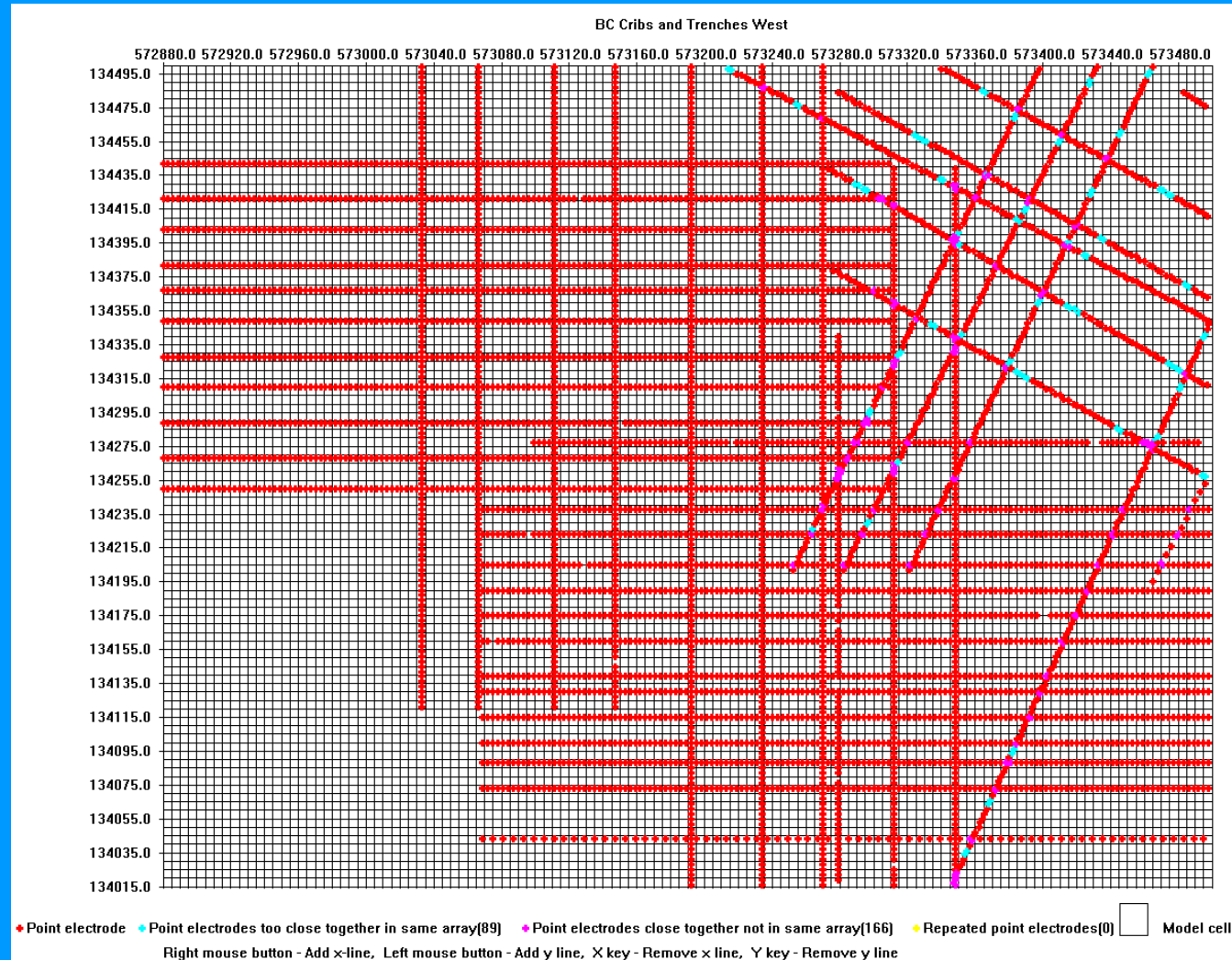
In many situations, it is not possible to have parallel surveys lines due to physical barriers such as rugged topography.

This example is from an I.P. mineral exploration survey. Note the use of remote electrodes for pole-dipole and gradient type arrays. The model grid is separated from the survey grid.



**Types of '3-D' surveys and models – complex case 2**

**Straight survey lines were used for an environmental survey in an area with flat terrain. There are lines running in different directions, and gaps due to cultural structures.**



# Smoothness constrained least-squares method

The equation for the smoothness-constrained least-squares inversion method is given by

$$\left[ \mathbf{J}_i^T \mathbf{R}_d \mathbf{J}_i + \lambda_i \mathbf{W}^T \mathbf{R}_m \mathbf{W} \right] \Delta \mathbf{r}_i = \mathbf{J}_i^T \mathbf{R}_d \mathbf{g}_i - \lambda_i \mathbf{W}^T \mathbf{R}_m \mathbf{W} \mathbf{r}_{i-1}$$

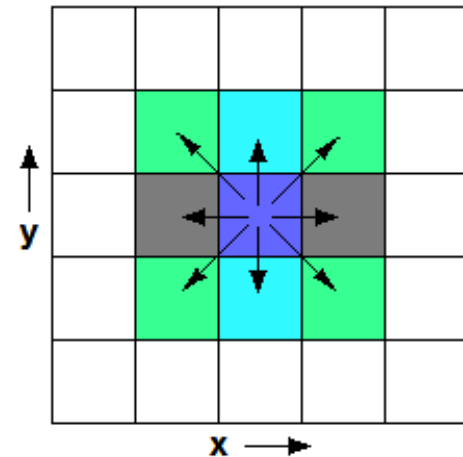
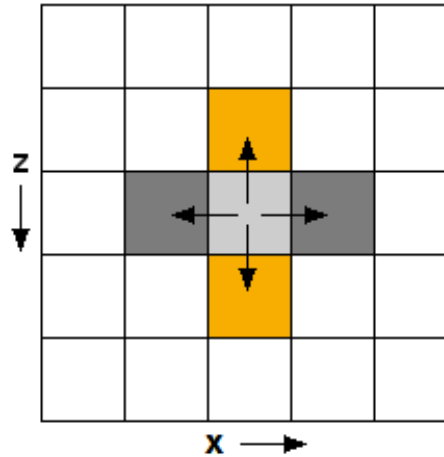
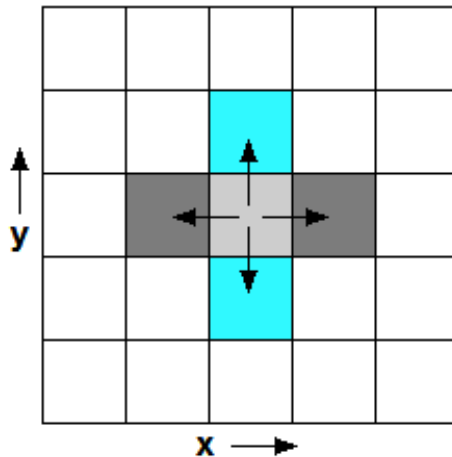
The roughness filter  $\mathbf{W}$  minimizes the change the resistivity between adjacent model cells in the x, y and z directions.  $\lambda$  is a damping factor,  $\Delta \mathbf{r}$  is the change in model resistivity values, and  $\mathbf{g}$  is the data misfit.  $\mathbf{J}$  is the Jacobian matrix of partial derivatives.  $\mathbf{R}_d$  and  $\mathbf{R}_m$  are weighting matrices for the L1-norm inversion method.

Coupling of 3-D model cells in roughness filter

Normal horizontal roughness filter x and y components

Normal vertical roughness filter with z component

Horizontal roughness with diagonal x-y components

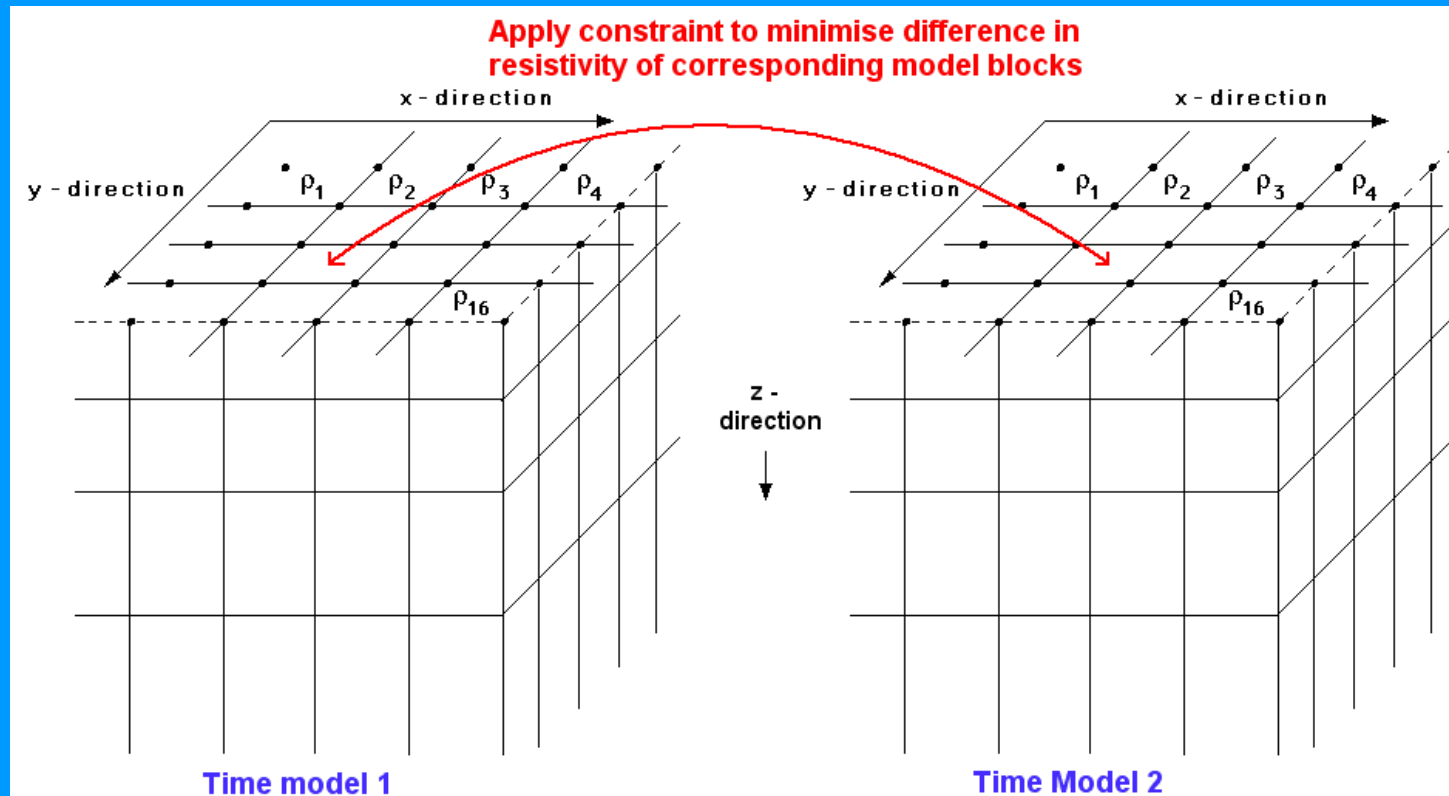


# Smoothness constrained time-lapse method

The smoothness-constrained least-squares method equation is modified to include a time-lapse constraint.

$$[\mathbf{J}_i^T \mathbf{R}_d \mathbf{J}_i + \lambda_i (\mathbf{W}^T \mathbf{R}_m \mathbf{W} + \alpha \mathbf{M}^T \mathbf{R}_t \mathbf{M})] \Delta \mathbf{r}_i = \mathbf{J}_i^T \mathbf{R}_d \mathbf{g}_i - \lambda_i (\mathbf{W}^T \mathbf{R}_m \mathbf{W} + \alpha_i \mathbf{M}^T \mathbf{R}_t \mathbf{M}) \mathbf{r}_{i-1}$$

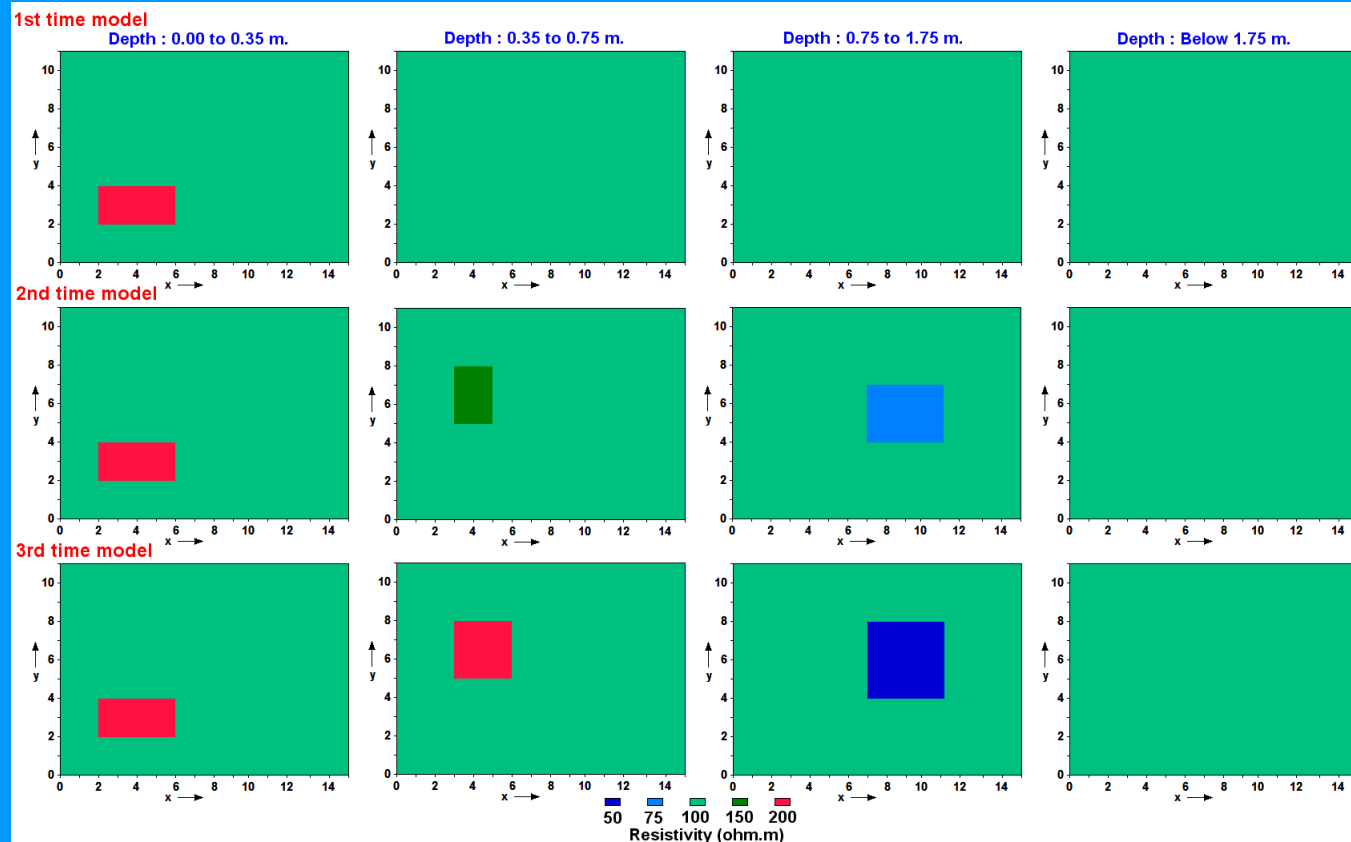
$\mathbf{M}$  is the difference matrix applied across the time models.  $\mathbf{R}_t$  is used to select between the L1 and L2 norm.  $\alpha$  is the temporal damping factor that gives the relative weight for minimizing the temporal changes.





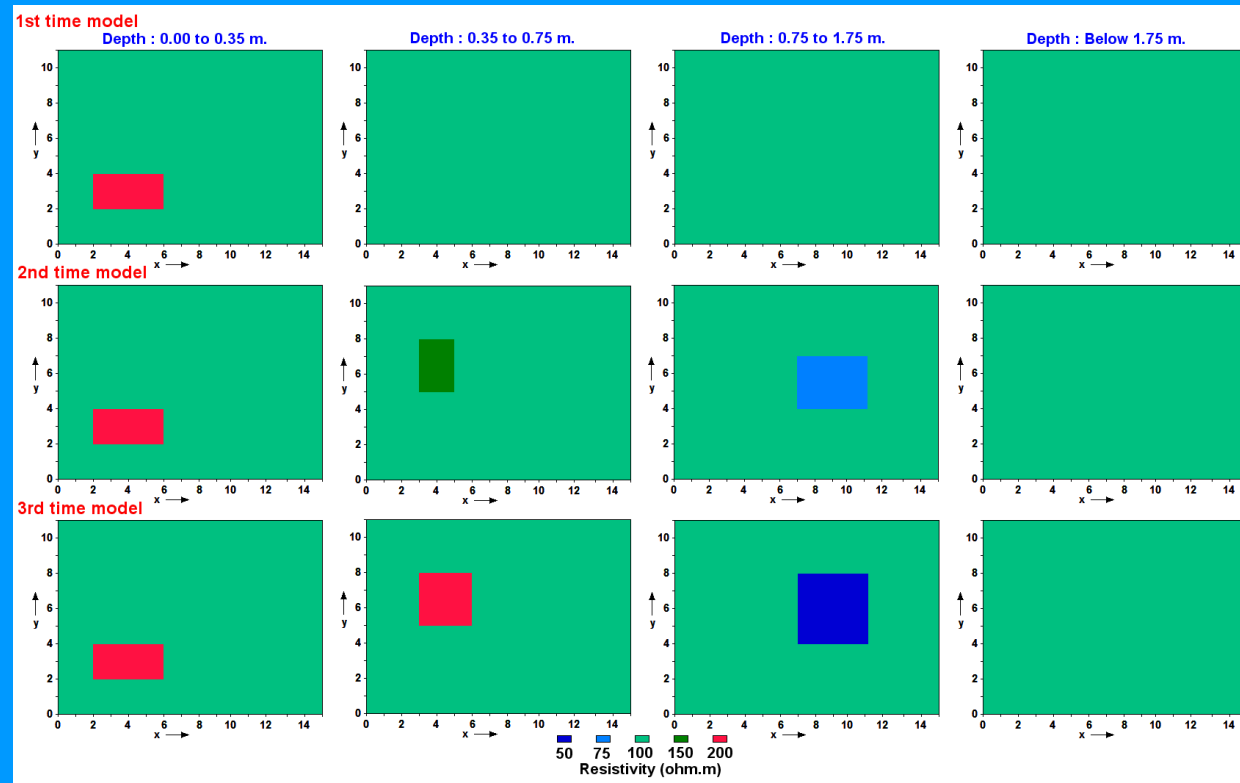
# Synthetic time-lapse test model

A test model with a 21 by 16 m survey grid is used. The 1st model has a single high resistivity block of 200  $\Omega\cdot\text{m}$  in the top layer in a medium of 100  $\Omega\cdot\text{m}$ . In the 2nd model, a high resistivity block of 150  $\Omega\cdot\text{m}$  is added in the second layer and a low resistivity block of 75  $\Omega\cdot\text{m}$  in the third layer. The sizes and resistivity contrasts of the deeper blocks are increased in the 3rd model.



# Synthetic time-lapse test model – data set

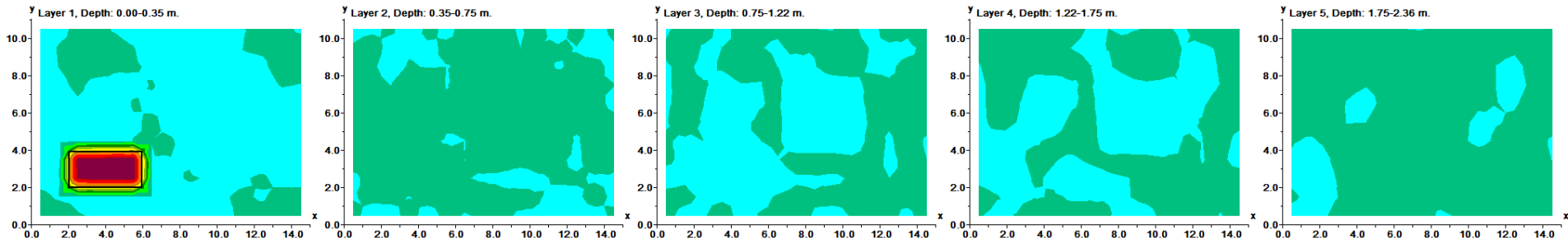
All the possible dipole-dipole measurements in both the  $x$  and  $y$  directions with a geometric factor of less than 1056 m. (corresponding to a dipole-dipole array with  $a=1$  m. and  $n=6$ ) are used in the test data set that has 2604 data points. Voltage dependent random noise with a maximum amplitude of 5% was added to the apparent resistivity values. The L1-norm was used for the model roughness and data misfit.



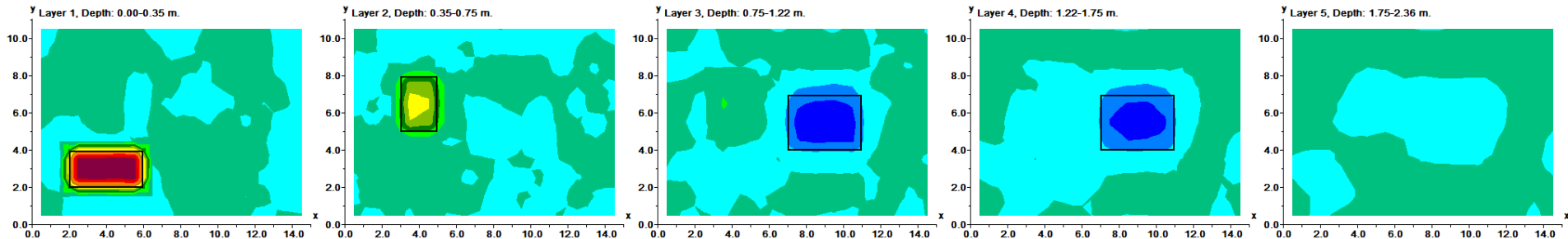
# Example inversion models

The sections below show the inversion models using a L2 norm time constraint. To better show the temporal changes, the percentage change in the resistivity between the 2<sup>nd</sup> and 3<sup>rd</sup> model with the 1st model is next used.

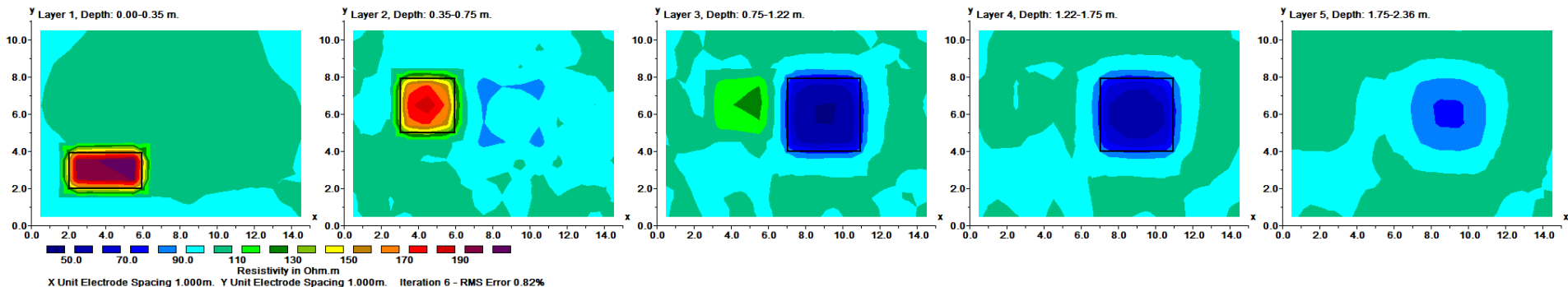
## 1st time inversion model



## 2nd time inversion model



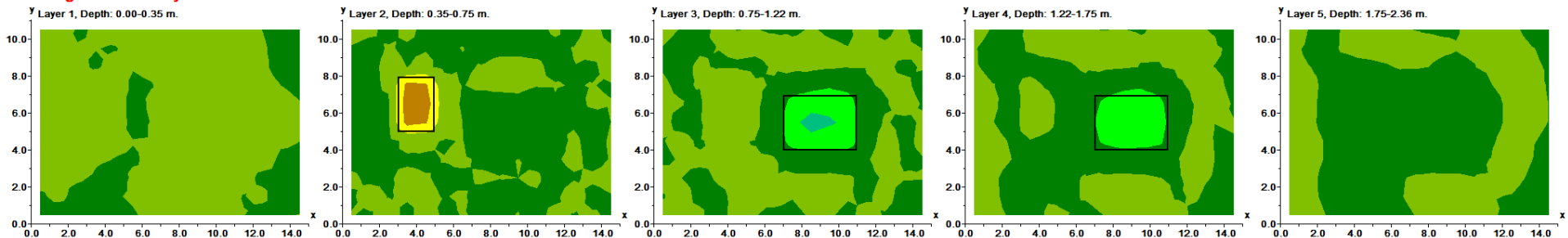
## 3rd time inversion model



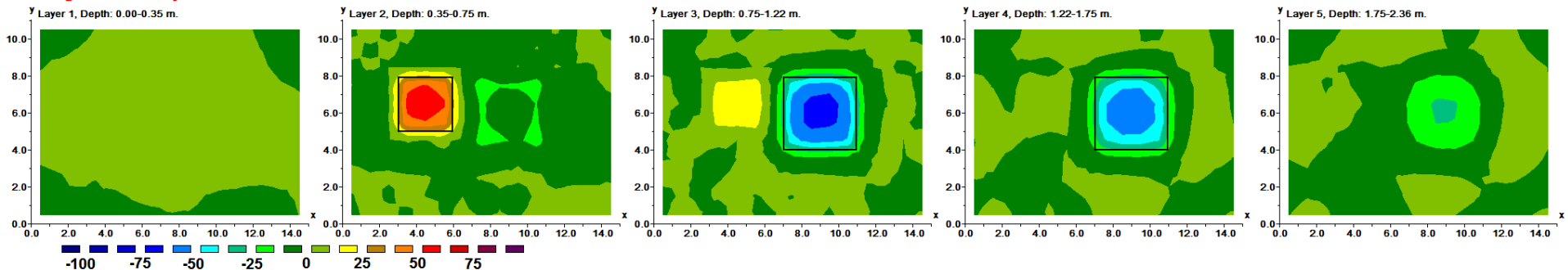
# Time difference sections – L2 norm temporal filter

The 2<sup>nd</sup> time model shows changes of +33% and -28% at the the two blocks (actual changes +50% and -50%). The 3<sup>rd</sup> time model shows changes of +60% and -68% (actual changes of +100% and -100%). The smaller amplitude of the changes in the inversion models is due to the use of the roughness filters to stabilize the inversion in the presence of noise. There is a 'leakage' of the high resistivity anomaly from the second layer to the third inversion model layer, and the low resistivity anomaly from the fourth to the fifth layer.

% change in resistivity between 2nd and 1st time models



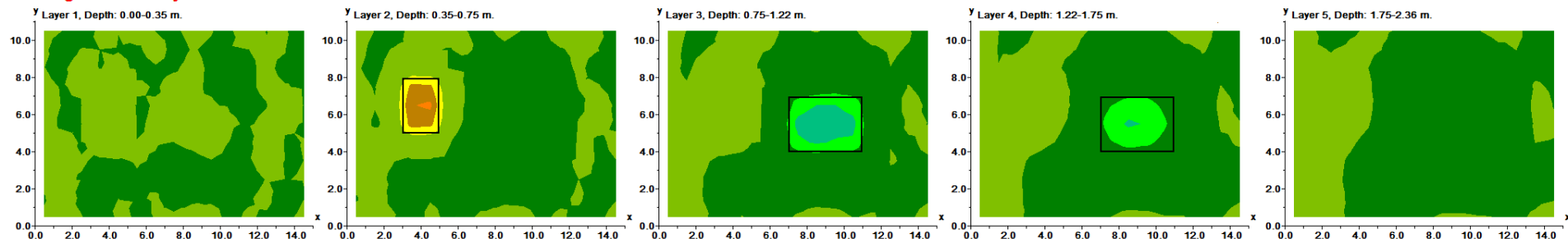
% change in resistivity between 3rd and 1st time models



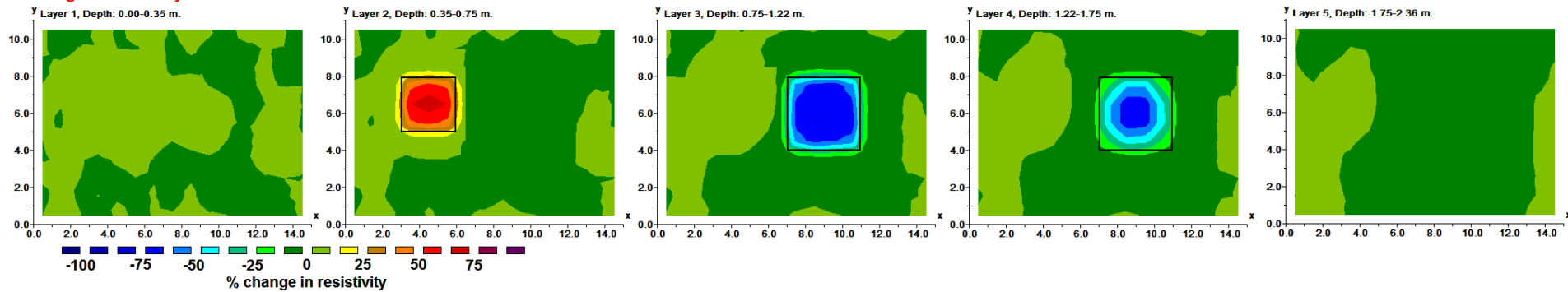
# Time difference sections – L1 norm temporal filter

The L1-norm filter produces a significant improvement in the models with changes of +40% and -36% for the 2<sup>nd</sup> time model (actual values +50% and -50%), and changes of +71% and -76% for the 3<sup>rd</sup> (actual values +100% and -100%). The two deeper blocks are also much better resolved. The 'leakage' of the low resistivity block into the fifth model layer is much reduced. There is a similar reduction in the 'leakage' of the high resistivity anomaly from the second to the third layer.

% change in resistivity between 2nd and 1st time models



% change in resistivity between 3rd and 1st time models

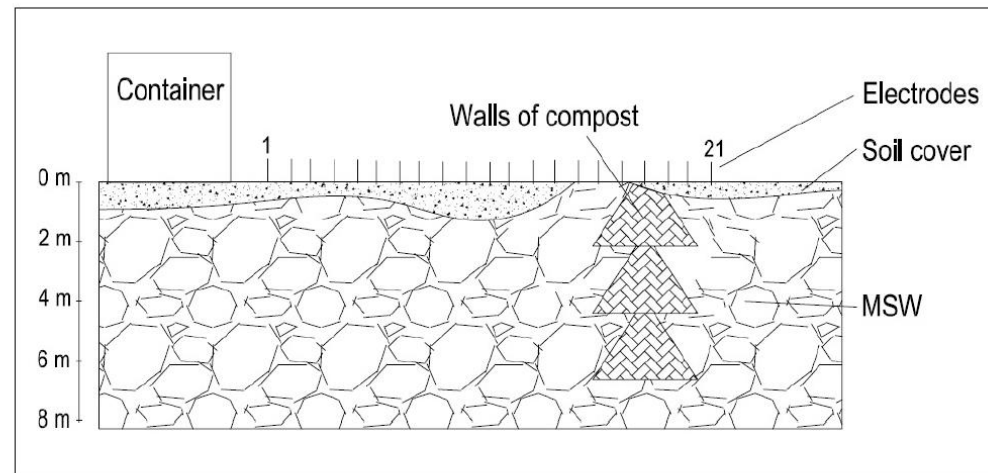


## Field data set –Landfill survey, Sweden

This survey was carried out to map methane gas accumulation in a landfill site in the Helsingborg area, Sweden. There were 9 parallel 2-D survey lines with 21 electrodes with a spacing of 1 m using the pole-dipole array. The spacing between the lines was 2 m. An inversion model with model cells of 1 m in both directions and diagonal roughness filters was used to reduce banding effects in the inversion. The inversion was carried out for two data sets measured on 18th and 27th August 2008 using a L1 norm time constraint.



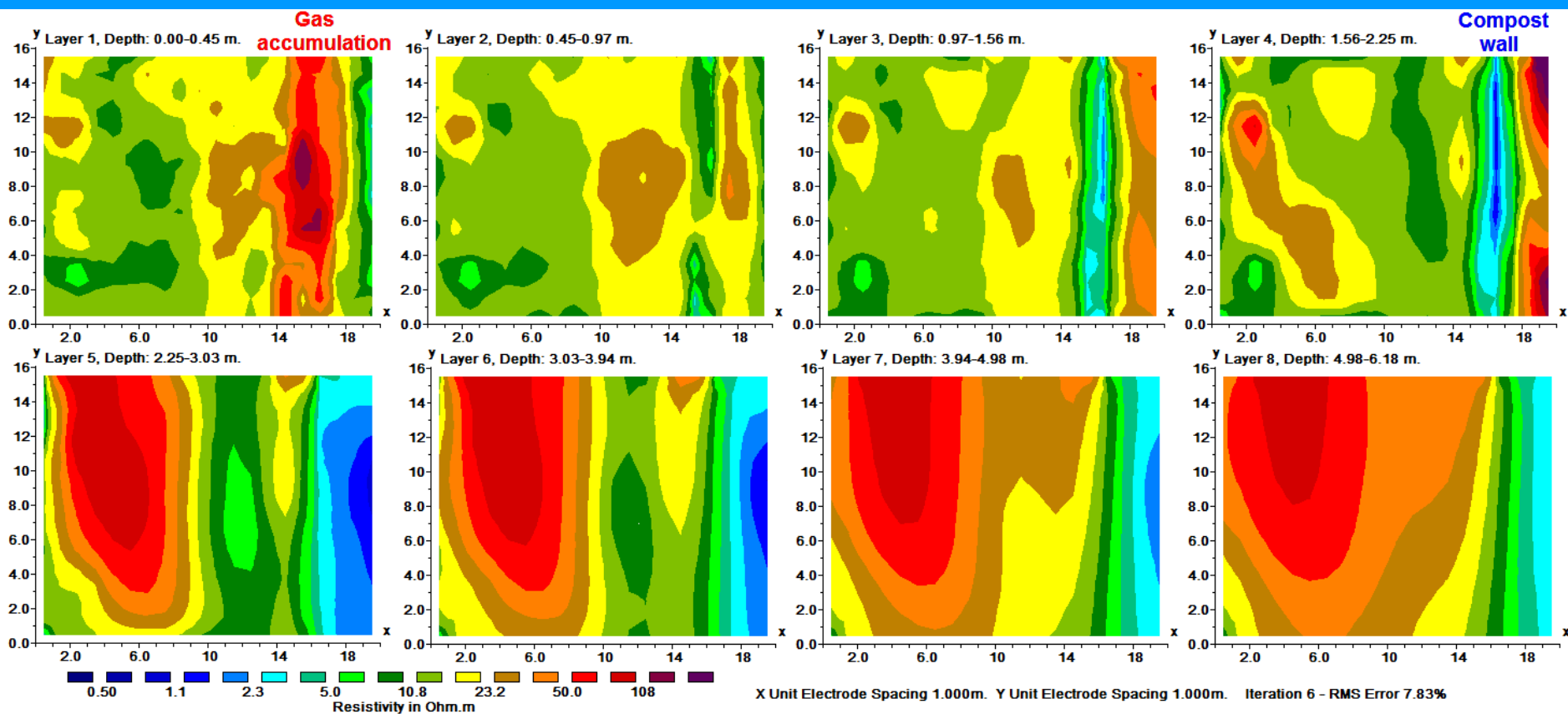
Photo showing the experimental site at the Filborna landfill.



Section of the experimental site at the Filborna landfill (sketch)

# Field data set – Helsingborg landfill survey, Sweden

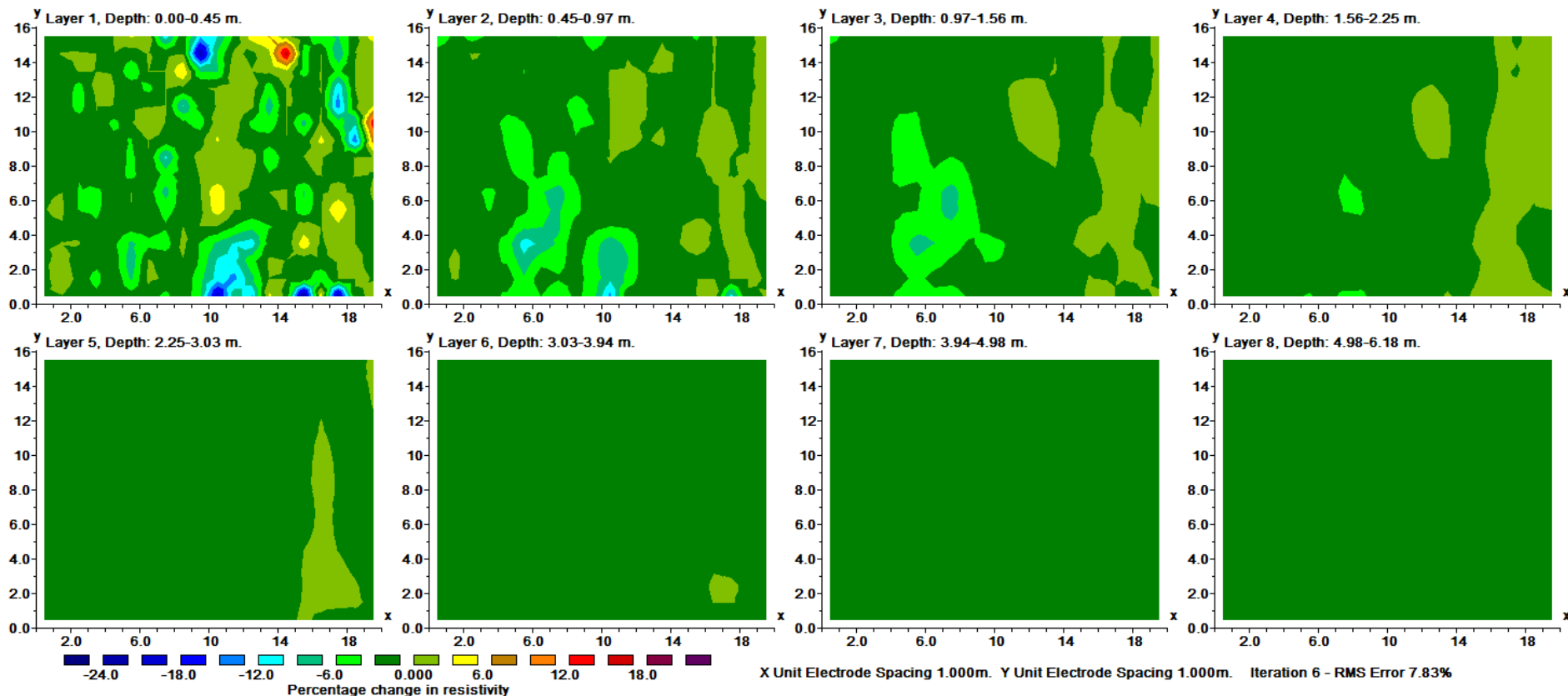
The 1<sup>st</sup> time inversion model shown below has areas with high methane concentration with higher resistivity values. The low resistivity linear feature on the right side of layers 3 and 4 corresponds to a subsurface compost wall consisting of soil and wood chips, while the high resistivity zone above it in layer 1 is believed to be gas that had migrated upwards through the wall.





# Helsingborg landfill survey difference section

The resistivity difference section show very little variations below a depth of 1.5 m. There are some minor near surface changes that could be caused by surface temperature variations that cause the gas to contract/expand as the temperature decreases/increases, and also changes in the landfill material moisture content.



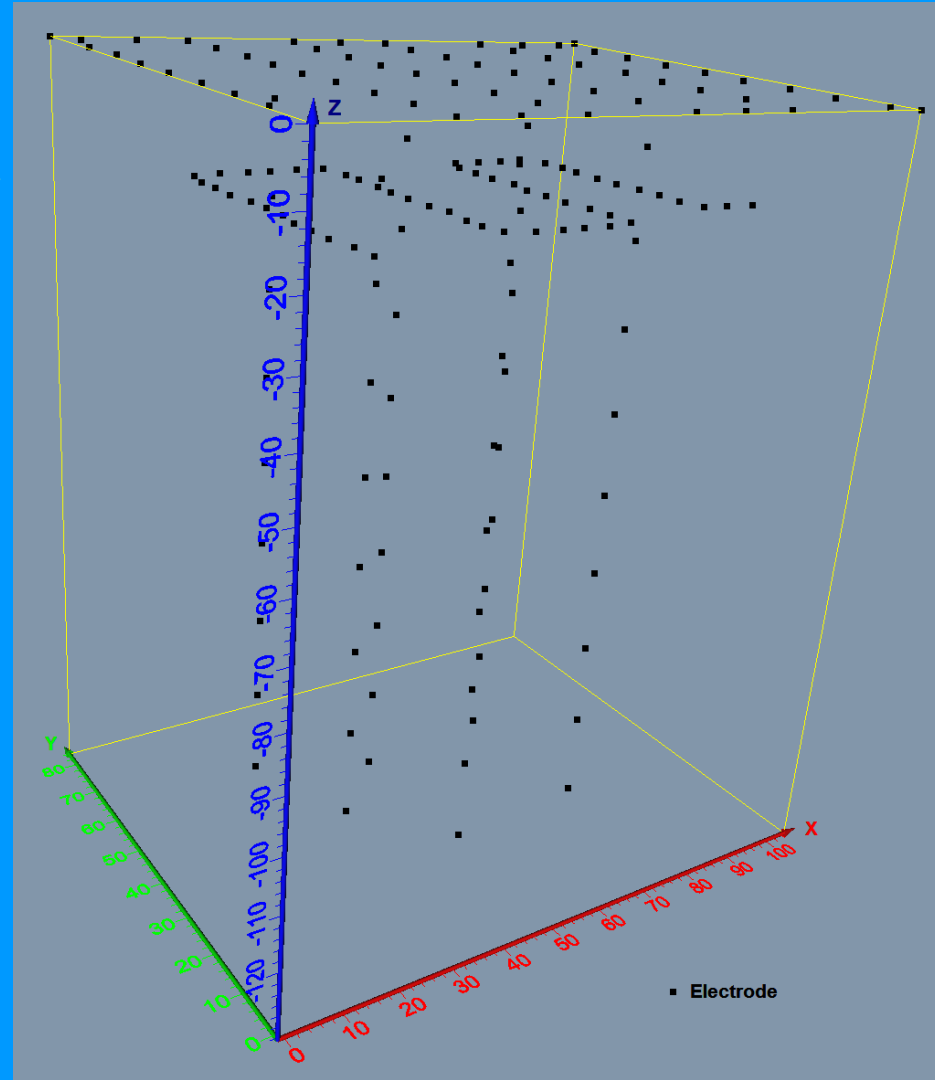


# Field data set – Irrigation experiment, USA

This survey used a grid of surface electrodes, a smaller set of electrodes at a depth of about 19 m, and along 6 boreholes up to about 130 m depth.

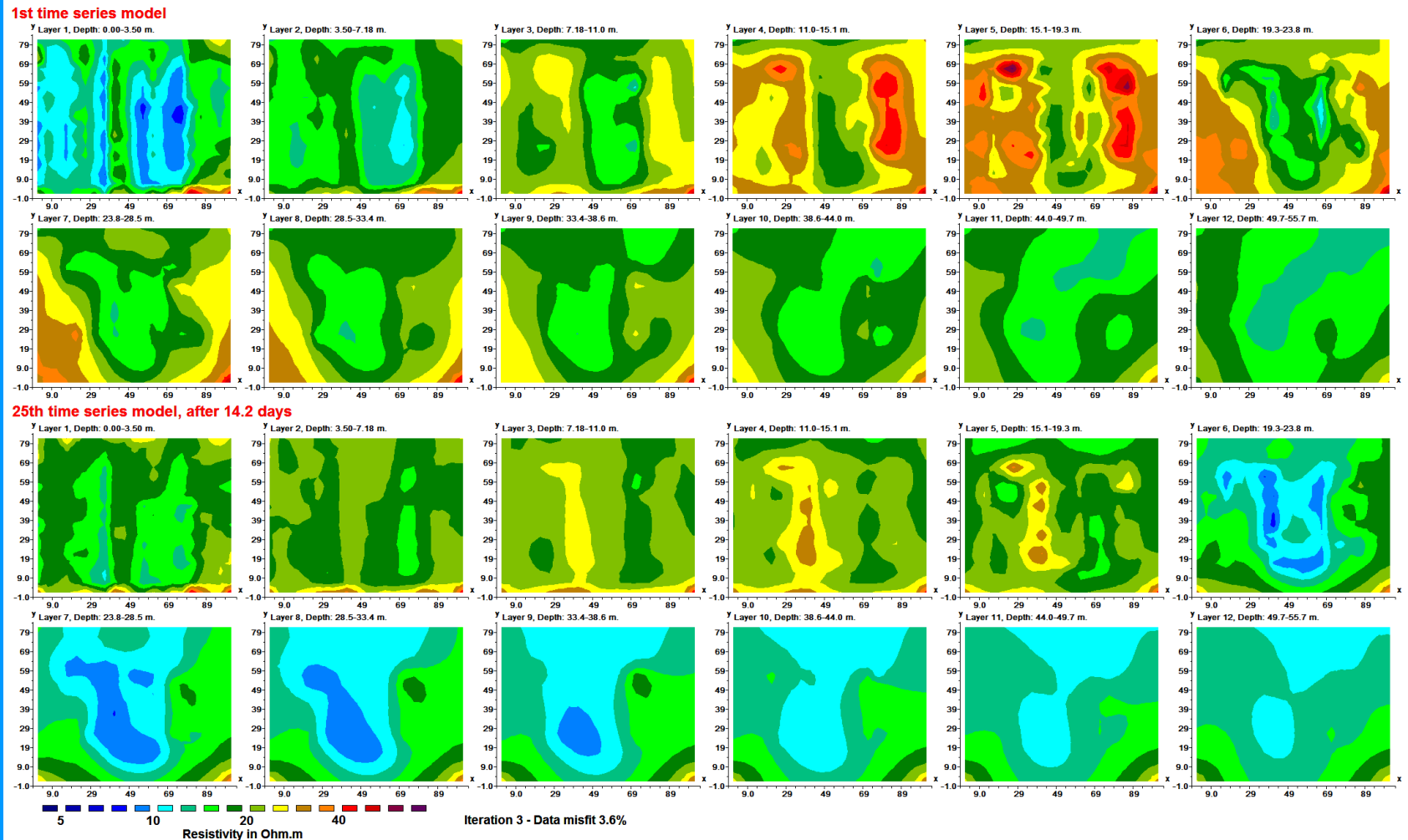
The experiment was conducted to study the feasibility of using 3-D time-lapse ERT to map the flow of electrolytes from the surface. Salt was added to the top soil layer as a marker.

Surface irrigation was applied to the ground surface and measurements were made about twice a day. Each data set has over 11600 data points, and the inversion model has about 8200 cells.



# Irrigation experiment - 1<sup>st</sup> and 25<sup>th</sup> time model sections

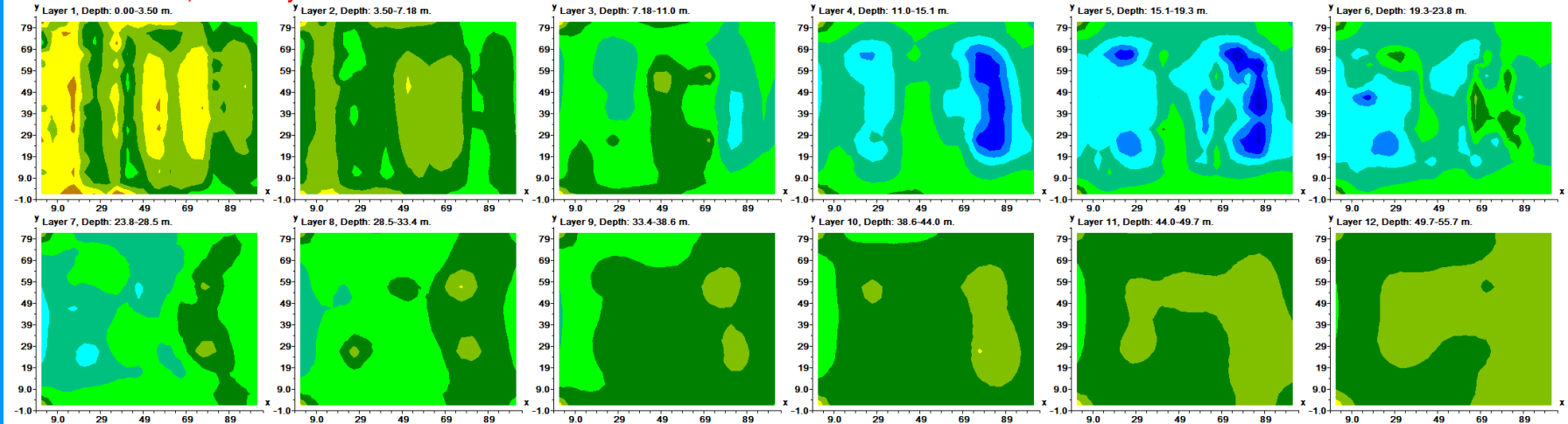
The inversion has 50 time data sets and models. In two of the model sections shown below, the resistivity in the upper layers increases while it decreases in the lower layers as the fluid migrates downwards after 14.2 days.



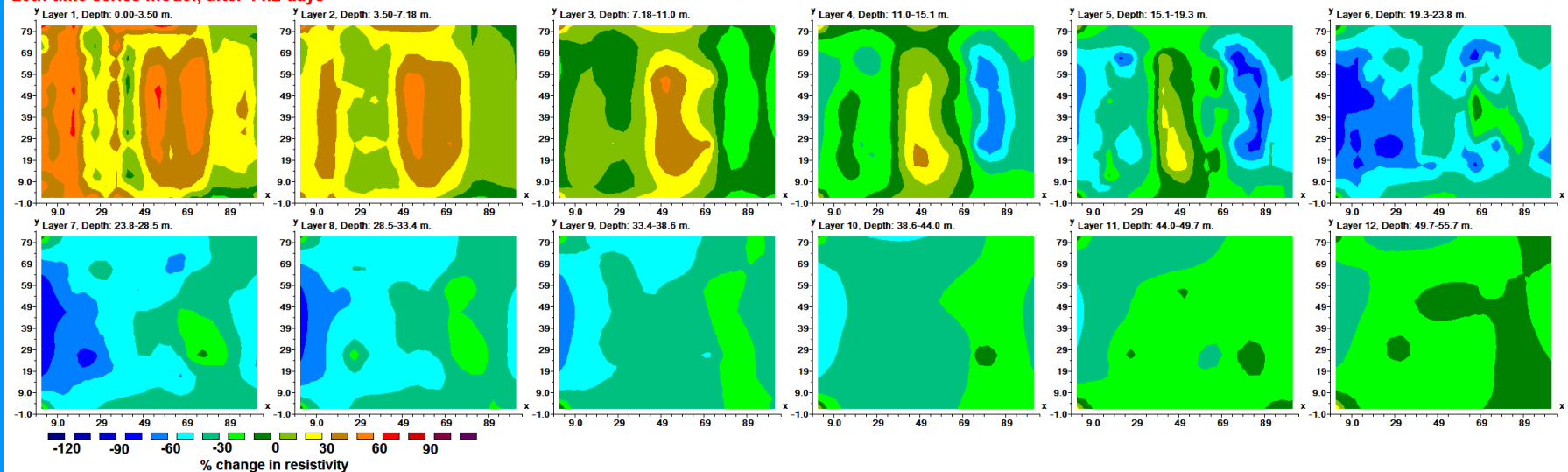
# Irrigation experiment - time difference models

The sections below (with percentage change in the resistivity values compared to the 1<sup>st</sup> model) show most of the fluids have migrated to 11-19 m depth after 1.7 days and to 19-28 m after 14.2 days.

4th time series model, after 1.7 days

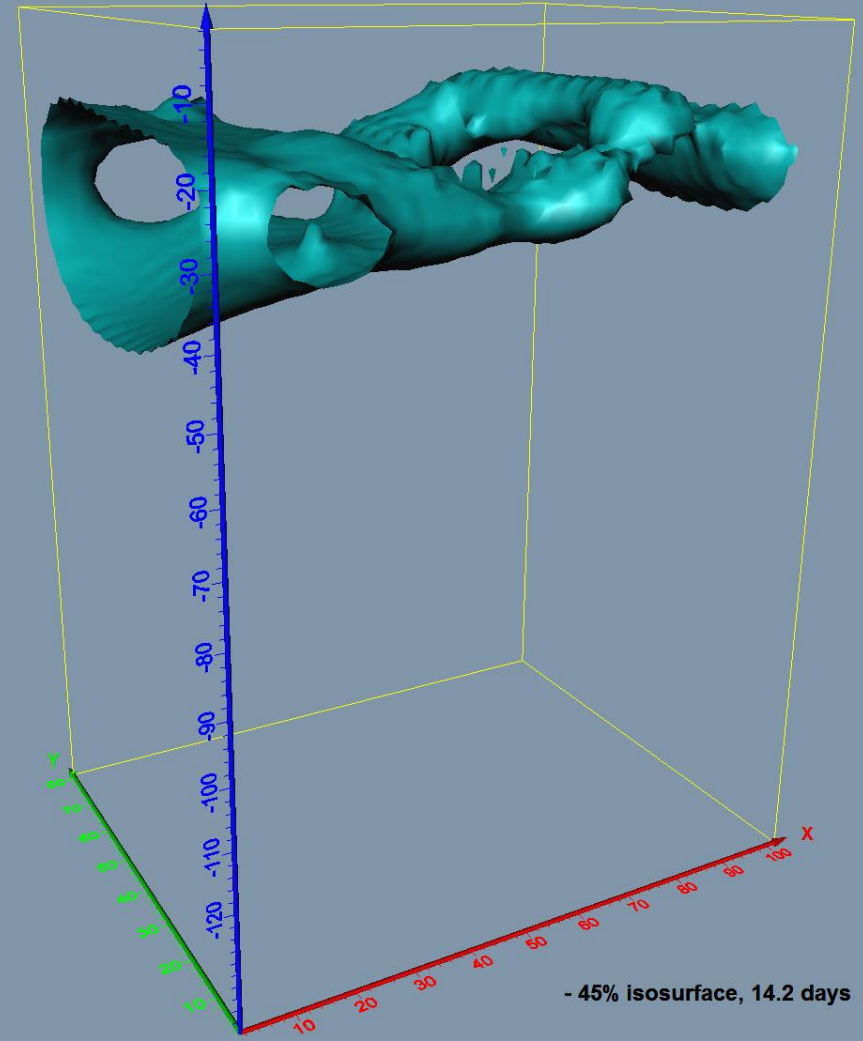
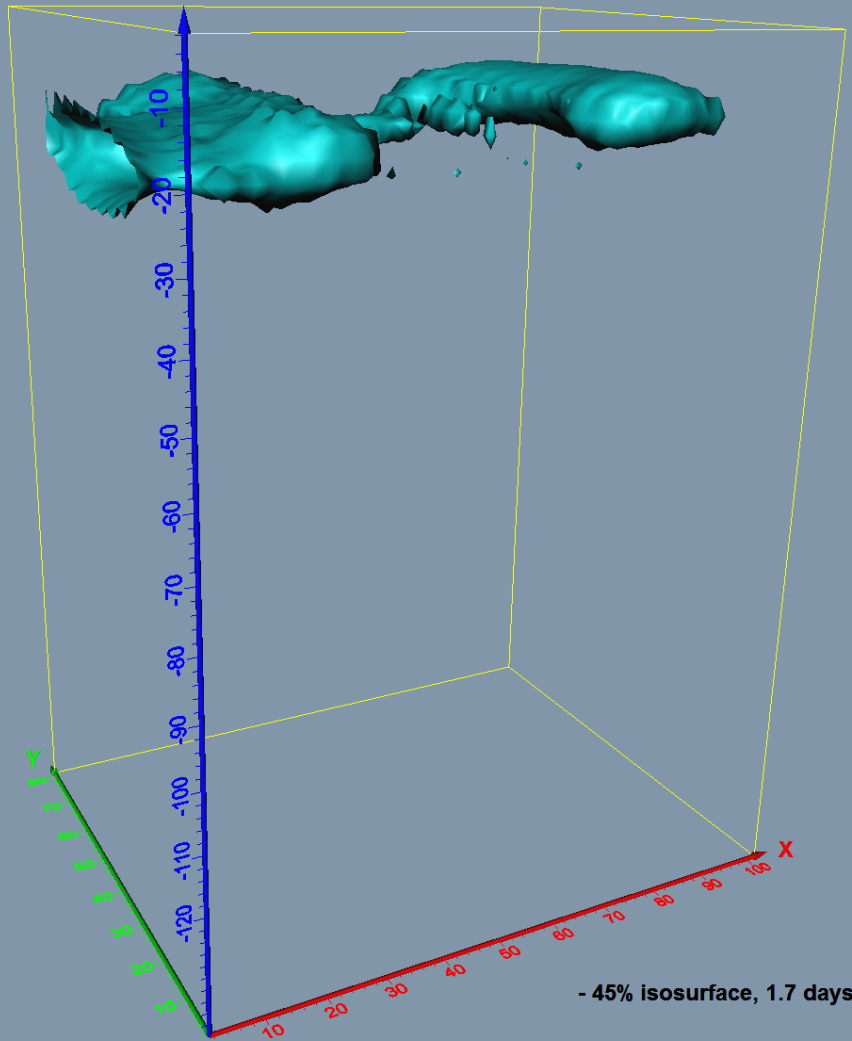


25th time series model, after 14.2 days



### 3-D plots of resistivity change for 1.7 and 14.2 days

Between 1.7 and 14.2 days, the low resistivity zone (with over 45% decrease in the resistivity) has spread and covers a greater volume as the fluids migrate downwards and sideways.



# Time plot of resistivity change for up to 28 days

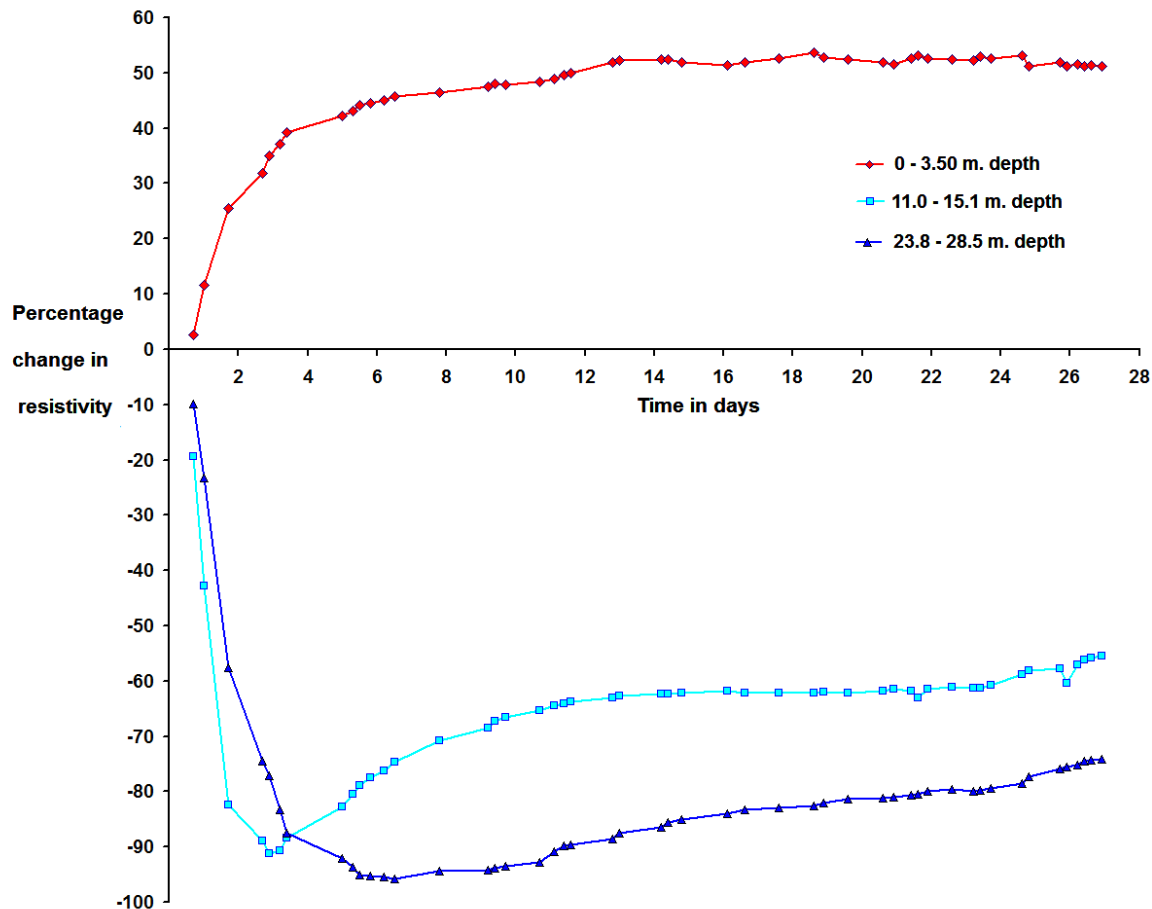
The resistivity for a model cell in the topmost layer increases as the dissolved salts from it migrate downwards. The middle layer shows a sharp minimum at 2.5 days, while the deeper layer has a broad minimum at 6 days as the fluids spreads sideways and downwards at a slower rate. The resistivity change with time is highly non-linear.

PC : 3.2 GHz 6-core i7, 24 GB RAM.

Data > 580,000 data points

Model > 410,000 cells

Computer time ~ 12 hours



# Conclusions

The constrained time-lapse method can successfully recover temporal changes in the resistivity even in the presence of noise for 3-D resistivity surveys. The L1-norm temporal constraint significantly improves the results when the resistivity changes abruptly with time.

An inversion of field data from a landfill site show changes in the resistivity of the materials above 1.5 meters depth. They are probably due to surface temperature variations that cause changes in the methane gas volume and moisture content within the landfill material near the surface.

A time-lapse 3-D survey over a period of 28 days using surface and subsurface electrodes successfully imaged both the lateral and vertical migration of dissolved salts from a surface irrigation experiment. As the fluids migrate downwards and laterally, the rate of movement slows down with increasing time and depth.